The Lithium−Sodium−Methylamine System: Does a Low-Melting Sodide Become a Liquid Metal?

Marc G. DeBacker,*,† El Bachir Mkadmi,† François X. Sauvage,† Jean-Pierre Lelieur,† Michael J. Wagner,‡,§ Rosario Concepcion,‡,⊥ Jineun Kim,‡,∥ Lauren E. H. McMills,# and James L. Dye*,‡

Contribution from LASIR-HEI CNRS LP2631, 13 rue de Toul, 59046 Lille Cedex, France, and Department of Chemistry and Center for Fundamental Materials Research, Michigan State University, East Lansing, Michigan 48824

Received August 4, 1995[⊗]

Abstract: The properties of the simplest sodide, $LiNa(CH_3NH_2)_n$, are reported as a function of n. The phase diagram, established by using differential thermal analysis, shows the presence of a compound with $n \approx 6$, which melts congruently at 168.5 ± 0.5 K. Two eutectics are present with $n = 7.3 \pm 0.3$, $T_1 = 166 \pm 1$ K and $n = 3.0 \pm 0.2$, $T_2 = 151 \pm 1$ K. The phase diagram was extended to metal concentrations that correspond to $n = 1.45$ and indicated the presence of a second compound with $2 \leq n \leq 3$. The properties of these systems were investigated by EPR and alkali metal NMR spectroscopies and static magnetic susceptibilities. The ^{23}Na NMR results clearly show that sodium is present as Na^- for $n \geq 8$. At higher metal concentrations the resonance line shifts smoothly toward more paramagnetic values (positive), with larger shifts at higher temperatures. EPR spectroscopy shows a transition from a single nearly symmetric line at large values of n to a strongly asymmetric signal characteristic of conduction electron spin resonance (CESR) when $n \leq 5$. The line shapes were fit by theoretical expressions and showed that liquid $LiNa(CH_3NH_2)_4$ has a conductivity comparable to that of liquid $Li(CH_3NH_2)_4$, a near metal.

Introduction

Alkali metals are very soluble in liquid ammonia.[1−3] These solutions are metallic at metal mole fractions of 0.04 and higher. Lithium is the only alkali metal that forms a defined compound, $Li(NH_3)_4$, with ammonia. It is a metal in both the liquid and solid states, with $\sigma = 16\,000\ \Omega^{-1}\ cm^{-1}$ for the liquid.[4]

Except for lithium, the solubility of alkali metals in simple alkylamines is much lower. In methylamine, $Li(CH_3NH_2)_4$ is formed; the phase diagram,[4−7] electrical,[8−10] and magnetic properties[11] have been studied. The electrical and magnetic behavior of $Li(CH_3NH_2)_4$ is that of a near metal in the liquid state ($\sigma \sim 400\ \Omega^{-1}\ cm^{-1}$)[9] and of a semiconductor in the solid state.[12] The solubility of lithium in ethylamine is also very high: samples of stoichiometry $Li(C_2H_5NH_2)_2$ have been observed, although only the compound $Li(C_2H_5NH_2)_5$ has been confirmed.[13] In this case, however, there is no hint of a metallic transition, and the system can be considered as a liquid "dielectride", *i.e.* a concentrated solution of paired solvated electrons.

Direct dissolution of alkali metals in aliphatic amines leads to the formation of dilute solutions of alkalides. It is now known[14] from the optical spectra of metal solutions in ethylenediamine[15] that sodium solutions contain primarily the ions Na^+ and Na^-, while potassium, rubidium, and cesium solutions are mixtures of solvated electrons and of the corresponding alkali metal anions in equilibrium. Upon solvent removal, the alkali metal anions and cations recombine, yielding the starting metals. This disproportionation into M^+ and M^- has never been observed for lithium solutions; only solvated electrons and lithium cations can be detected and Li^- does not seem to exist in solution. When sodium cations are added to solutions that contain other alkali metal anions or solvated electrons in amines, the sodide anion always forms.[16] The reaction of sodide solutions with other alkali metal cations never produces the other alkalides, indicating that the sodide anion is much more stable than other alkalide ions or solvated electrons.

The synthesis of crystalline alkalides requires the presence of molecules such as crown ethers or cryptands (C) that form

† LASIR−HEI CNRS LP2631.
‡ Michigan State University.
§ Present address: Department of Chemistry, Massachusetts Institute of Technology, Cambridge, Massachusetts 02139.
⊥ Present address: Department of Sciences, Pontificia Universidad Católica Madre y Maestra, Santiago, Dominican Republic.
∥ Present address: Department of Chemistry, Gyeongsang National University, Chinju, 660-701, Korea.
Present address: Department of Chemistry, Ohio University, Athens, Ohio 45701.
⊗ Abstract published in *Advance ACS Abstracts,* February 15, 1996.

(1) Symons, M. C. R. *Q. Rev.* **1959**, *13*, 99−115.
(2) Das, T. P. In *Advances in Chemical Physics*; Prigogine, I., Ed.; Wiley: New York, 1962; Vol. 4, pp 304−388.
(3) Thompson, J. C. *Electrons in Liquid Ammonia*; Oxford University Press: Oxford, 1976.
(4) Yamamoto, M.; Nakamura, Y.; Shimoji, M. *Trans. Faraday Soc.* **1971**, *67*, 2292−2297.
(5) Yamamoto, M.; Nakamura, Y.; Shimoji, M. *Trans. Faraday Soc.* **1971**, *68*, 135−139.
(6) Nakamura, Y.; Horie, Y.; Shimoji, M. *J. Chem. Soc., Faraday Trans. 1* **1974**, *70*, 1376−1383.
(7) Hagedorn, R.; Lelieur, J. P. *J. Phys. Chem.* **1980**, *84*, 3652−3654.
(8) Edwards, P. P.; Lusis, A. R.; Sienko, M. J. *J. Chem. Phys.* **1980**, *72*, 3103−3112.
(9) Toma, T.; Nakamura, Y.; Shimoji, M. *Philos. Mag.* **1976**, *33*, 181−187.
(10) Hagedorn, R.; Sienko, M. J. *J. Phys. Chem.* **1982**, *86*, 2094−2097.
(11) Edwards, P. P.; Buntaine, J. R.; Sienko, M. J. *Phys. Rev. B* **1979**, *19*, 5835−5846. Page, C. J.; Johnson, D. C.; Edwards, P. P.; Holton, D. M. *Z. Phys. Chem.* **1994**, *184*, 157−172.
(12) Stacy, A. M.; Johnson, D. C.; Sienko, M. J. *J. Chem. Phys.* **1982**, *76*, 4248−4254.
(13) De Backer, M. G.; Mkadmi, E. B.; Sauvage, F. X.; Lelieur, J.-P.; Wagner, M. J.; Concepcion, R.; Eglin, J. L.; Guadagnini, R. A.; Kim, J.; McMills, L. E. H.; Dye, J. L. *J. Am. Chem. Soc.* **1994**, *116*, 6570−6576.
(14) DeBacker, M. G.; Dye, J. L. *J. Phys. Chem.* **1971**, *75*, 3092−3096.
(15) Dewald, R. R.; Dye, J. L. *J. Phys. Chem.* **1964**, *68*, 128−134.
(16) Dye, J. L.; DeBacker, M. G.; Eyre, J. A.; Dorfman, L. M. *J. Phys. Chem.* **1972**, *75*, 839−846.

0002-7863/96/1518-1997$12.00/0

complexes with alkali cations.[17,18] The overall process may be written as:

$$2M(s) + C(s) \xrightarrow{\text{solvent}} M^+C + M^- \xrightarrow{\text{crystallization}} (M^+C)\cdot M^-(s) \quad (1)$$

These compounds are bulky and the distance between the anions is dictated by the size of the complexed cation. All of the "classical" sodides (and other alkalides) that have been reported to date are ionic salts of the alkali metal anions,[19] and none shows metallic conductivity. In order to study the effects of possible overlap of the wave functions of the highly polarizable alkali metal anions, simpler systems that contain the lithium cation solvated by small molecules were investigated.

Large concentrations of sodium can be obtained in amines by using concentrated lithium−methylamine solutions to dissolve sodium metal.[20] Optical and NMR spectra suggested that when equimolar amounts of lithium and sodium metal are put together in the presence of a simple amine (methylamine or ethylamine), a reduction of sodium atoms by lithium takes place, producing the alkali metal anion Na^-. Note that sodium alone is virtually insoluble in ethylamine and in higher alkylamines and its solubility is only of the order of 10^{-3} M in methylamine.

The driving force for the solubilization of sodium by lithium is provided by the complexation of the lithium cation by the amine. This Li^+−methylamine "complex" also plays the role of a charge separator to prevent the recombination of ions and the precipitation of metal. These systems are representative of *liquid alkalides* in which solvent molecules play the role of complexant.

Liquid sodides based upon the complexation of lithium cations by amine molecules have been previously reported. With ethylenediamine, the compound $Li^+(NH_2CH_2CH_2NH_2)_2\cdot Na^-$ can be isolated as a bright yellow-gold solid that metls at 250 K and decomposes or decomplexes at 273 K.[21] The existence of the compound $Li^+(C_2H_5NH_2)_4\cdot Na^-$ was recently established[13] and the phase diagram of this system was determined. However, in spite of the very high concentration of the alkali metals, no hint of electronic conductivity could be detected. This sodide is apparently just a salt with a very low melting point. In the same study, it was also shown that lithium was extremely soluble in ethylamine but that no metallic compounds were formed; systems of composition $Li(C_2H_5NH_2)_n$ with n as small as five could be viewed as liquid electrides with most electron spins paired.

The simplest system involving lithium, sodium, and amines should be $LiNa(NH_3)_n$. However, no such compounds can be detected and Na^- is not formed in ammonia[13] although Na^- forms in mixtures of methylamine and ammonia (molar ratio 1:1) as evidenced by the presence of its visible absorption peak at 660 nm.[22]

In this work, we describe the simplest sodide, obtained with equimolar mixtures of lithium and sodium in methylamine, $LiNa(CH_3NH_2)_n$. The phase diagram obtained by differential thermal analysis (DTA) is presented as a function of n and the approximate compositions of up to three new compounds are established. Alkali metal NMR and EPR spectroscopy provide information about the occurrence of an electronically conducting liquid phase with near-metallic character.

The EPR spectra are analyzed in terms of formalisms that were previously used for concentrated metal ammonia solutions and for lithium−methylamine solutions.[23−25] When the solutions being studied are electronically conducting, the EPR line shape is asymmetric, indicating the presence of conduction electrons. In such CESR studies,[8,11,26] the A/B ratio of the low- to high-field peak heights of the first derivative EPR spectrum has been frequently used to analyze asymmetric curves, especially when there is evidence for the presence of conduction electrons. When A/B is larger than 2.5, the line shape can be interpreted in terms of a "dysonian" formalism.[27,28] These calculations were extended by Webb[29] to the case of spherical metallic particles. This expression was further simplified in the case of particle sizes smaller than ten times the skin depth[30] and was shown to be applicable to the CESR spectrum of small potassium particles for which the A/B ratio was only of the order of 1.2.[31]

Experimental Section

Since alkali metal solutions in amines are thermodynamically unstable, rigorous sample preparation procedures must be followed. The decomposition reaction is catalyzed by a variety of substances such as iron oxide, traces of precious metals, and the walls of the cell if they are not properly passivated. Furthermore, alkalide compounds react with oxygen and/or moisture. Lithium and sodium metal were handled in a glovebox filled with dry argon or helium with removal of oxygen and nitrogen. The masses of the metals were determined to within 0.1 mg. Prior to making a solution, the metals were dissolved in anhydrous liquid ammonia that was then slowly removed. The metals were then evacuated to less than 10^{-5} Torr at room temperature for at least 12 h to remove all traces of ammonia. This procedure yields the metals in a finely dispersed reactive state. Methylamine and ammonia (Union Carbide) were purified by forming a blue solution with either lithium or sodium−potassium alloy for several days. The solvent was then stored in a separate vessel. The amount of methylamine was determined by gas volumetric methods followed by condensation. The samples were prepared at low temperature (200 K) by letting the solvent and the metals remain in contact for several days. The samples were vigorously shaken at regular intervals at a slightly higher temperature (250 K) to ensure complete dissolution of both metals.

NMR studies were carried out with a Bruker WH 180 spectrometer. The resonance frequencies of ^7Li and ^{23}Na were 69.95 and 47.62 MHz, respectively (field = 4.2277 T). Reported chemical shifts are relative to $Li^+(aq)$ and $Na^+(aq)$ at infinite dilution and were determined by comparison with 0.1 M aqueous solutions of $LiClO_4$ and NaCl. The temperature was regulated by passing the dry N_2 spinning gas through a liquid N_2 heat exchanger and heating it with an in-line heater. The temperature was monitored with a thermocouple placed in the N_2 stream immediately ahead of the entrance to the spinner.

Static susceptibilities were measured with an SHE Corp. Model 800 SQUID susceptometer that can reach temperatures as low as 2 K. The samples were contained in sealed fused silica containers that were suspended in the susceptometer. After the measurements were perfored, the samples were allowed to decompose at room temperature and were run again. This procedure allows subtraction of the diamagnetic

(17) Dye, J. L.; Lok, M. T.; Barnett, B. L.; Tehan, F. J. *J. Am. Chem. Soc.* **1974**, *96*, 608−609.
(18) Tehan, F. J.; Barnett, B. L.; Dye, J. L. *J. Am. Chem. Soc.* **1974**, *96*, 7203−7208.
(19) Dye, J. L.; DeBacker, M. G. *Annu. Rev. Phys. Chem.* **1987**, *38*, 271−301.
(20) Faber, M. K.; Fussa-Rydel, O.; Skowyra, J. B.; McMills, L. E. H.; Dye, J. L. *J. Am. Chem. Soc.* **1989**, *111*, 5957−5958.
(21) Concepcion, R.; Dye, J. L. *J. Am. Chem. Soc.* **1987**, *109*, 7203−7204.
(22) Blades, H.; Hodgins, J. W. *Can. J. Chem.* **1955**, *33*, 411−425.
(23) Glaunsinger, W. S.; Sienko, M. J. *J. Magn. Reson.* **1973**, *10*, 253−262.
(24) Damay, P.; Leclercq, F.; Devolder, P. *J. Phys. Chem.* **1984**, *88*, 3760−3764.
(25) Edmonds, R. N.; Harrison, M. R.; Edwards, P. P. *Annu. Rep. Prog. Chem. Sect. C: Phys. Chem.* **1985**, *82*, 265−308.
(26) Catterall, R.; Mott, N. F. *Adv. Phys.* **1969**, *18*, 665−679.
(27) Feher, G.; Kip, A. F. *Phys. Rev.* **1955**, *98*, 337−347.
(28) Dyson, F. J. *Phys. Rev.* **1955**, *98*, 349−359.
(29) Webb, R. H. *Phys. Rev.* **1967**, *158*, 225−233.
(30) Berim, G. O.; Cherkasov, F. G.; Kharakhashyan, E. G.; Talanov, Y. I. *Phys. Status Solidi A* **1977**, *40*, K53−K55.
(31) Guy, S. C.; Edmonds, R. N.; Edwards, P. P. *J. Chem. Soc., Faraday Trans. 2* **1985**, *81*, 937−947.

Table 1. ^{7}Li and ^{23}Na NMR Chemical Shifts (in ppm) for $Li^{+}(CH_3NH_2)_nNa^{-}$

		chemical shift				
nucleus	T (K)	$n = 4$	$n = 6$	$n = 8$	$n = 12$	$n = 16$
^{7}Li	253	9.0	6.0	3.2	2.3	2.5
	233	7.4	4.8	2.7	2.0	2.2
	213	5.6	4.0	2.3	2.1	2.1
	203		3.7	2.2	2.1	2.1
^{23}Na	253	1.9	−26.7	−50.7	−58.9	−58.0
	233	−10.4	−33.9	−53.5	−59.5	−59.0
	213	−21.8	−41.3	−55.8	−59.9	−59.6
	193		−43.0	−56.2	−60.1	−59.8

contribution of the container and the initial sample,[32] even when gaseous decomposition products are formed.

The methods used to prepare samples for EPR work are described elsewhere.[33] It should be mentioned, however, that special care had to be taken in order to have homogeneous solutions in the EPR tube. All transfers were made at low temperatures under isothermal conditions. Spectra were recorded on a Bruker ESP 300 spectrometer at X-band. The temperature was controlled by a stream of cold nitrogen regulated to ±1 °C.

The equipment used for DTA measurements has been previously described.[13] The sample volumes were of the order of 2 mL. This quantity of solution allowed accurate determination of the composition of the sample while giving correct DTA curves. The sample temperature was measured with an accuracy of 0.1 °C and the difference in temperature was measured to within 0.01 °C.

Results

When lithium and sodium metals are dissolved in methylamine, solvated lithium sodide is formed. The appearance of this salt in solution is indicated by the modification of the color, which goes from a deep blue color for the lithium solutions that are formed first to the bright bronze-gold color of lithium sodide. The existence of this salt requires the presence of amines. When all the solvent is removed under vacuum the metals are recovered as bright silvery sponges or films. If the whole process is carried out at temperatures of 240 K or lower, there are no traces of decomposition products. Concentrated solutions are very viscous and opaque, and they tend to stick to the glass. Thin films on the walls of the cell are blue by transmission and gold-bronze by reflection; their optical absorption spectrum shows the peak at 660 nm characteristic of Na^{-}.[20]

The ^{7}Li and ^{23}Na NMR spectra each consist of one symmetric peak. The line width of the ^{23}Na peak is ∼100 Hz at temperatures higher than 190 K. Below that temperature, the system behaves as a frozen sample and the line width increases to ∼530 Hz. The values of the ^{23}Na chemical shift in liquid $Li^{+}(CH_3NH_2)_nNa^{-}$ for $n = 4$, 6, 8, 12, and 16, as recorded at several temperatures, are reported in Table 1. For the more dilute systems ($n = 12$, 16) and for all solid samples, the position of the ^{23}Na resonance line corresponds to that of isolated Na^{-} in other sodides.[34] It is almost temperature independent. For more concentrated liquid samples (n = 8, 6, and 4), the resonance line is paramagnetically shifted and its chemical shift is temperature dependent. The position of the ^{7}Li resonance peak depends in a similar way on the concentration and temperature but the shift is less pronounced.

DTA curves show the presence of solid−solid transitions as well as the melting temperature of the compounds. The detection of the various peaks and their areas as a function of composition can be used to determine the stoichiometries of the species responsible for the various transitions. Thermograms were recorded starting from the lowest temperature to avoid undercooling. The shapes of the DTA curves depend on the heating rate. Low scanning rates were used to separate closely spaced peaks; 0.2 °C/min was a typical value used in this work. Typical DTA curve shapes obtained at selected concentrations are shown in Figure 1. The temperatures of the transitions are given as a function of composition in Figure 2, and the areas under the peaks corresponding to the two eutectic halts are shown in Figure 3. The composition−temperature data are given in Table 2.

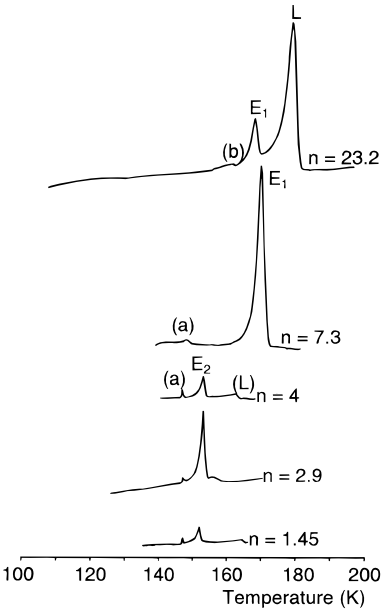

Figure 1. Selected DTA curves for $LiNa(CH_3NH_2)_n$. E_1 and E_2 are the peaks corresponding to the two eutectics, L denotes the liquidus and a and b are solid−solid transitions.

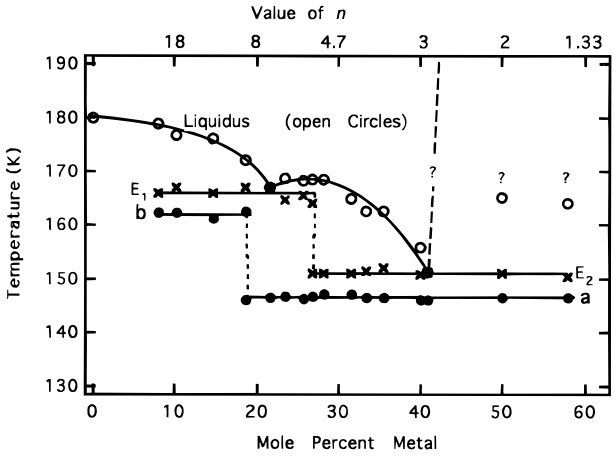

Figure 2. Experimental compositions and temperatures associated with transitions of $LiNa(CH_3NH_2)_n$. This figure serves as a tentative phase diagram since the various transitions are identified. The two dashed lines on the left represent approximate locations of compounds and that on the right represents the presumed saturation line. A compound presumably exists between $n = 3$ and 2.

For dilute systems ($n > 9$), two pronounced endothermic peaks are observed. The first one (E_1) corresponds to a solid−liquid transition attributed to the melting of a eutectic at 166 ± 1 K, while the other one (L) corresponds to the liquidus. The eutectic melting temperature is invariant with respect to metal concentration, while the liquidus temperature increases in the usual manner as the metal concentration decreases. A small, poorly defined peak, which corresponds to a solid−solid transition (b) at 162 ± 0.5 K, disappears for $n \leq 9$. In the

(32) Landers, J. S.; Dye, J. L.; Stacy, A.; Sienko, M. J. *J. Phys. Chem.* **1981**, *85*, 1096−1099.

(33) Mkadmi, E. B. Ph.D. Dissertation, Université des Sciences et Technologies de Lille, France, 1993.

(34) Ellaboudy, A.; Dye, J. L. *J. Magn. Reson.* **1986**, *66*, 491−502.

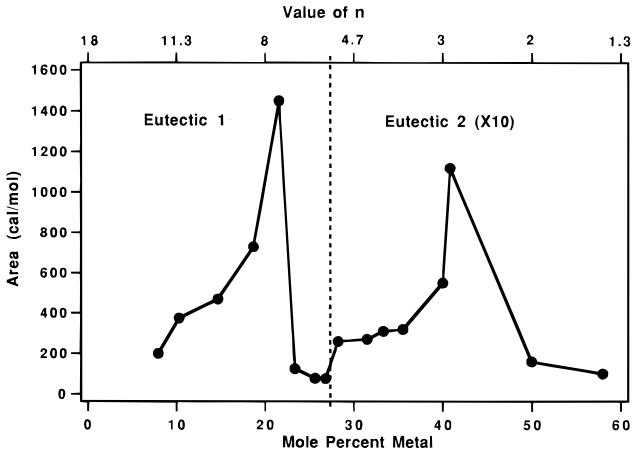

Figure 3. Variations of the areas under the eutectic peaks as a function of composition of $LiNa(CH_3NH_2)_n$. The dashed line separates the data for the two eutectics. Note the difference in vertical scales for the two regions.

Table 2. Temperatures (K) of Endothermic Transitions from Differential Thermal Analysis

conc (MPM)	value of n	solid−solid T_a	eutectic T_{e2}	liquidus T_L	eutectic T_{e1}	solid−solid T_b
57.97	1.45	146.6	150.4	164.2		
50	2	146.6	150.9	165.1		
40.82	2.9	146.1	151.1	151.1		
40	3	146.2	150.7	155.8		
35.52	3.63	146.6	152.0	162.7		
33.33	4	146.6	151.5	162.6		
31.49	4.35	147.1	150.9	165.0		
28.25	5.08	147.1	150.9	168.7		
26.84	5.45	146.7	150.9	168.7	164.1	
25.64	5.8	146.4		168.4	165.7	
23.44	6.53	146.7		168.8	164.8	
21.6	7.26	146.6		167.1	167.1	
18.67	8.71	146.1		172.3	167.2	162.6
14.7	11.61			176.2	166.0	161.4
10.3	17.42			176.9	167.2	162.4
7.93	23.22			179.0	166.0	162.4
0				180.0		

intermediate range ($5.5 < n < 9$), the eutectic peak E_1 is still observed but it disappears for $n < 5.5$. A new solid−solid transition (a), characterized by a low-intensity peak, is observed at 146.5 ± 0.5 K for all values of $n < 8.7$.

In concentrated systems that melt completely ($3 \leq n \leq 5.5$), the DTA curves show 3 peaks: one in the solid state that corresponds to the solid−solid transition previously observed (a), a new peak (E_2) attributed to a solid−liquid transition (melting of the second eutectic), and a liquidus. The second eutectic has a melting temperature of 151 ± 1 K, independent of concentration.

The intersections of the liquidus curves with the eutectic halts shown in Figure 2 yield compositions of the two eutectics of $n = 7.3 \pm 0.3$ and 2.9 ± 0.3. As shown in Figure 3, the areas under the first eutectic peak as a function of composition are very small near the maximum in the second liquidus curve at $n = 5.5 \pm 1.0$. An abrupt drop occurs in the area under E_1 between $n = 7.3$ and 6.5, suggesting the presence of a compound near $n = 6$. These results show unequivocally the presence of at least one compound with a congruent melting temperature of 168.5 ± 0.5 K. The drop in the area under the eutectic peak suggests the nominal formula $Li^+(CH_3NH_2)_6{\cdot}Na^-$ while the switch from one eutectic temperature to another is more consistent with the formula $Li^+(CH_3NH_2)_5{\cdot}Na^-$. Information about other possible compounds is discussed later.

Alkalides are diamagnetic since the alkali metal anions have an ns^2 electronic configuration. The temperature dependence

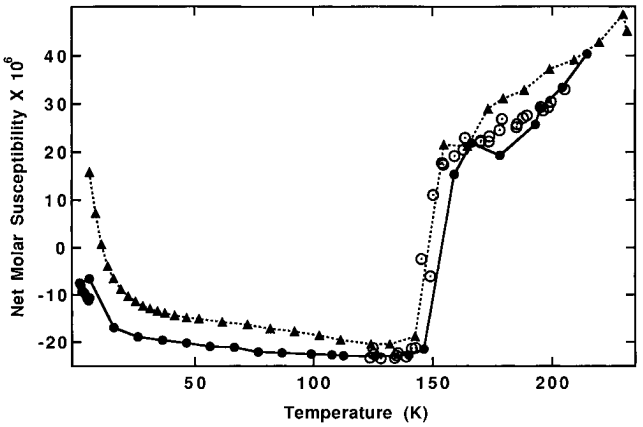

Figure 4. Temperature dependence of the static magnetic susceptibility of $LiNa(CH_3NH_2)_4$. The data points have been corrected by subtracting the signal due to the sample tube and the decomposed sample. The dashed line and triangles correspond to heating from 5 K after sudden cooling, while the solid line and filled circles refer to decreasing temperature. The open circles were obtained last during heating.

of the net static magnetic susceptibility, after subtraction of the contribution from the container and the decomposed sample, is shown in Figure 4 for a concentrated sample of composition $LiNa(CH_3NH_2)_4$. Data were obtained both after a quench to 5 K and during slow cooling from 240 to 2 K. In the solid state the sample is essentially diamagnetic, but there is a sharp increase in paramagnetism at the melting point. The susceptibility continues to increase as the temperature is raised, indicating partial dissociation to Na^- to yield solvated electrons.

Although the samples are intrinsically diamagnetic, there are enough defect electrons to give rise to an EPR spectrum. EPR spectra were recorded as a function of temperature for concentrations corresponding to $n = 4$, 5, 6, 8, 12, and 16. Studies of solutions more concentrated than $n = 4$ were not attempted since the homogeneity of the sample inside the EPR tube was uncertain. All samples were inserted into the EPR cryostat as liquids at ~220 K and frozen rapidly *in situ*. After stabilization at the lowest available temperature, the temperature was gradually increased. This procedure was chosen in order to avoid undercooling, but it probably did not allow the system to come to equilibrium in the solid state. Similar to the results obtained from EPR studies of concentrated lithium−methylamine systems,[35] they are strong microwave absorbers. This required that only a small part of the sample could be placed in the microwave cavity; thus, it was not possible to evaluate the number of spins via double integration of the EPR spectrum. As a result, this study is based on line shape analysis rather than on intensity comparisons. At temperatures higher than 240 K, the tuning of the cavity was lost in the neighborhood of resonance, which limited the accessible temperature range.

All EPR spectra corresponding to $n \geq 6$ ("dilute systems") are very similar. Their major characteristic is a single line situated at the free electron g-value. In the solid state, the most important feature is a single symmetrical narrow line with ΔH_{pp} of the order of 0.2 G. A smaller broader signal sometimes coexisted with this narrow peak, but it could only be detected by using high modulation amplitudes. It usually disappeared in the vicinity of the temperature of the solid−solid transition, b. Its magnitude (and even its existence) is strongly dependent upon the thermal history of the sample. Upon melting, there was a sudden large increase of the intensity of the signal that required moving the sample out of the cavity in order to be able to tune the cavity. For all concentrations ($n \geq 6$) there

(35) Buntaine, J. R.; Sienko, M. J.; Edwards, P. P. *J. Phys. Chem.* **1980**, *84*, 1230−1232.

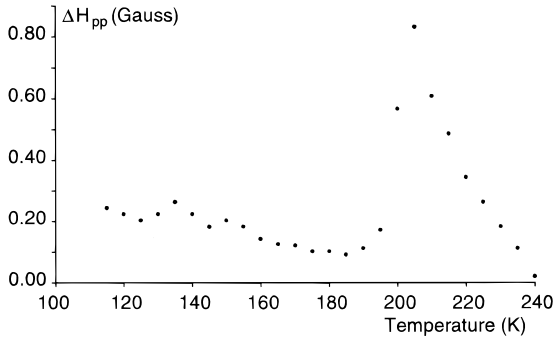

Figure 5. Variation of the EPR line width, ΔH_{pp}, with temperature for $LiNa(CH_3NH_2)_6$. Note the sudden increase upon melting followed by a gradual decrease. The intensity also increased markedly upon melting and then remained constant.

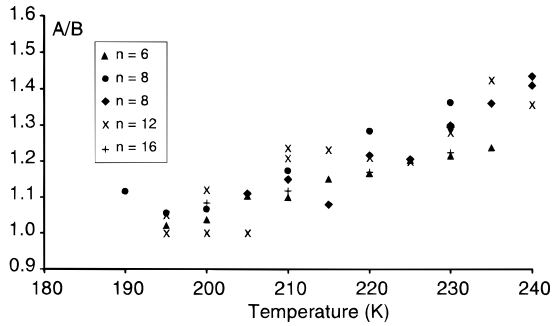

Figure 6. Variation of the ratio of the low-field to high-field EPR derivative peak amplitudes, *A/B*, as a function of temperature for $LiNa(CH_3NH_2)_n$ for $n \geq 6$. For the solid (temperatures below 180 K) *A/B* is close to 1.0.

was also a sudden increase in the peak width, ΔH_{pp}, as shown in Figure 5 for $n = 6$. As the temperature increased, the line narrowed and the line shape began to become asymmetric. The temperature dependence of *A*/*B* is shown in Figure 6 for all samples with $n \geq 6$. Note that the line is nearly symmetrical up to 205 K, but that *A*/*B* increases gradually at higher temperatures for all samples.

For more concentrated samples ($n = 4$ and 5) in the solid state, two EPR peaks were observed at the lowest temperature, but a broad peak disappeared at about 145 K (the temperature of transition *a* shown in Figure 2) to leave only a single, very weak symmetric narrow line. When the temperature reached the liquidus point (170 K) the intensity increased markedly and the line became strongly asymmetric with a "dysonian" shape. This phenomenon was sudden and reversible. For comparison purposes, a lithium sample of $Li(CH_3NH_2)_4$ was also prepared under the same conditions as in this study. Its EPR spectrum was also asymmetric, but broader and with a different temperature dependence as shown by the comparison of T_2 values in Figure 7.

Discussion

All the transitions observed in the DTA experiments are endothermic. An exothermic signal observed below the melting point in the related system lithium−sodium−ethylamine[13] was not observed in this case. The experimental but incomplete phase diagram for the system lithium−sodium−methylamine is shown in Figure 2. It is clear that its general features are very different from those of $Li(CH_3NH_2)_n$, in which the most concentrated system that could be reached corresponded to the value $n = 4.0$.[7] In the present case, higher concentrations of lithium (and of sodium) can be attained and liquid solutions with compositions as high as $LiNa(CH_3NH_2)_3$ can be formed. It is likely that a solid compound with an even higher metal concentration exists.

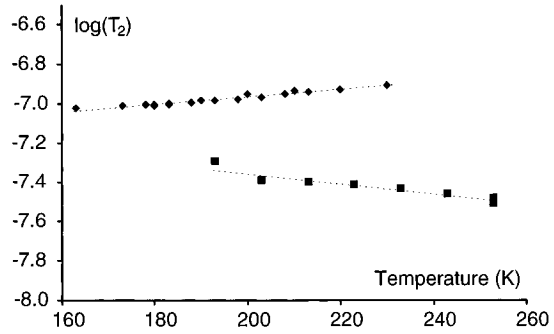

Figure 7. Variation of $\log(T_2)$ *vs* T for $Li(CH_3NH_2)_4$ (bottom line, squares) and for $LiNa(CH_3NH_2)_4$ (top line, diamonds). T_2 (=T_1) is the EPR transverse relaxation time obtained from fits of the data by the Webb equation.

The various domains present in the phase diagram (Figure 2) have been identified by the sudden disappearance of peaks as a function of concentration. The disappearance of the small peak labeled *b* at $n = 9$ together with the appearance of the peak labeled *a* suggests the formation of a compound $LiNa(CH_3NH_2)_9$, which exists only in the solid state and decomposes before melting. However, in view of the small magnitude of the DTA signals and the possibility of non-equilibrium in the solid state, the existence of this compound is uncertain. The presence of two eutectics, one vanishing as the other one appears, is characteristic of the existence of a defined compound that melts congruently. Its composition is $LiNa(CH_3NH_2)_n$ with $n = 5.5 \pm 1.0$. The sharp drop in the area under peak E_1 (Figure 3) between $n = 7.3$ and 6.5 suggests the formation of a compound with *n* between these values. However, the overlap of the eutectic peak with that of the liquidus makes this assignment uncertain. Without question, however, at least one solid compound exists between $n = 7.3$ and 5.0.

The composition of the second eutectic, $LiNa(CH_3NH_2)_3$, could result in the coordination number of four that is usually observed for compounds that contain Li^+, provided that a sodide anion replaced a solvent molecule. As it stands, the phase diagram is not complete in the highly concentrated region since the saturation line is not defined. Very small high-temperature peaks that cannot be attributed to the melting of the pure solvent or to that of any of the compounds suggest that there exists a compound to the right of the second eutectic but its position cannot be established. The abrupt drop in the area under the second eutectic peak between $n = 3$ and 2 suggests compound formation with $3.0 > n \geq 2.0$. If these systems contained a mixture of solid LiNa alloy and eutectic, a substantial peak at the eutectic temperature would be expected for $n = 2.0$. We *tentatively* suggest the formation of a compound $LiNa(CH_3NH_2)_2$ that does not melt, but undergoes a solid state transition at ~164 K.

Alkali metal NMR shows unambiguously that the species present in the liquid state cannot be only Li^+ and "normal" Na^- as was the case in other related systems.[13,21] Only on the dilute side are the major species clearly lithium cations and sodide anions. For $n \leq 8$, the position of the ^{23}Na resonance is gradually displaced toward paramagnetic values, becoming more pronounced as the temperature is increased. Only a single narrow line is observed, indicating either rapid exchange or a single paramagnetic environment. Therefore, even at compositions with *n* larger than that of the compound(s) near $n = 6$, there is evidence that Na^- is not isolated from perturbing effects. It seems reasonable to postulate that partial ionization of Na^- occurs and that the system might be described by the formula $Li^+(CH_3NH_2)_n(Na^-)_\delta(e^-)_{1-\delta} + (1 - \delta)Na°$, with $0 < \delta < 1$. The chemical shift response of Na^- suggests that either there is a rapid equilibrium, $Na^- \rightleftarrows Na° + e^-$, or the NMR peaks of

both Na^- and Li^- are shifted in the paramagnetic direction by interaction with the unpaired spins of e^-. Frozen samples show a broad peak of Na^- at its normal position (−60 ppm) which could result from "quenching" of the exchange mechanism or from the decrease in the concentration of unpaired electrons (observed upon solidification by both magnetic susceptibility and EPR measurements).

For concentrated systems, there is strong evidence that at least a fraction of the Na^- ions release electrons to the surrounding medium upon forming the liquid state. The static susceptibility goes suddenly from diamagnetic to a small paramagnetic value, and the electrons released can be trapped in the solid by a rapid quench to 5 K (Figure 4). Accompanying the melting there is a strong paramagnetic shift of the ^{23}Na NMR peak position, and most importantly, the EPR signal becomes strongly asymmetric with an A/B ratio of the order of 2.5. Comparison of the shapes of the lithium−sodium system with that of $Li(CH_3NH_2)_4$, prepared and studied under the same experimental conditions, shows that phase separation into the liquid electride and the sodide does not occur. The A/B ratio is similar in both cases, 2.41 and 2.53 for the LiNa and the Li systems, respectively, but ΔH_{pp} is larger ($T_1 = T_2$ is smaller) for $Li(CH_3NH_2)_4$ and shows the opposite temperature dependence (Figure 7).

In "dysonian" models, the ratio A/B is related to the ratio d/δ where d is the thickness of a metallic plate[27,28] or the diameter of a spherical particle[29] and δ is the classical skin depth. The skin depth is related to the microwave resistivity ρ by the relation:

$$\delta = \left(\frac{c^2 \epsilon_0 \rho}{\pi \nu}\right)^{1/2} \tag{2}$$

We have verified by non-linear least-squares methods[36] that none of the formalisms based on the Dyson model[27,28] of thick plates can give a reasonable fit to the experimental curves, even taking into account dielectric relaxation.[37] The best fit of the data was obtained with the formalism of Webb[29] applicable to samples having spherical symmetry. The equations are complex (and we have noted that the second-order terms are probably incorrect but in this application they are negligible). The Webb formulation to first order can be used here since $A/B < 4$, a region where the line shape does not depend on the ratio of the time needed for the electron to cross the skin depth (T_D) divided by the spin−lattice relaxation time ($T_2 = T_1$ in our case). Second-order terms in the Webb equation are not important in this region. The parameters that were adjusted in our least-squares fits of the data were d/δ, T_2, the position of the center of the field, and the amplitude of the signal. Almost perfect fits were obtained at all temperatures. A representative fit and a deviation plot are shown in Figure 8. The values of $\log(T_2)$ as a function of temperature are plotted for both $Li(CH_3NH_2)_4$ and $LiNa(CH_3NH_2)_4$ in Figure 7. For $Li(CH_3NH_2)_4$ there is a slight decrease with increasing temperature, while for $LiNa(CH_3NH_2)_4$ the slope is positive. In a systematic study of the variation of T_2 with temperature for a number of concentrated solutions of lithium in methylamine,[35] Buntaine concluded that the appearance of a metal to non-metal transition was characterized by a negative slope of the T_2 vs temperature curve. Our systems apparently are on the verge of the metallic state. For the LiNa system with $n = 4$ and 5, the value of d/δ is independent of temperature from the melting point to 213 K to within 1%, although freezing and thawing a sample with $n = 4$ caused up to a 4% increase. The latter behavior is not unexpected since the effective sample size could change in the process.

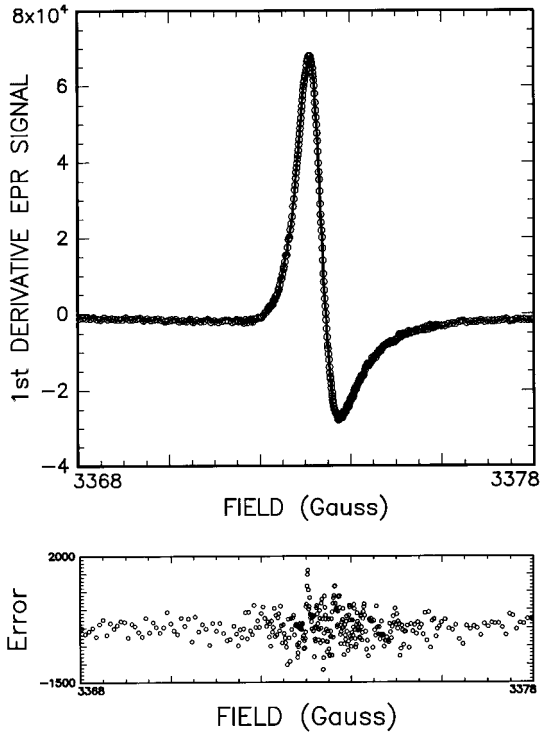

Figure 8. Non-linear least-squares fit of the EPR spectrum of $LiNa(CH_3NH_2)_5$ at $T = 203$ K by the Webb equation. The bottom graph shows the deviation from the least-squares fit.

Samples of $LiNa(CH_3NH_2)_n$ having $n \geq 6$ would be diamagnetic if they contained only the species Li^+ and Na^-. The observed EPR signals must therefore correspond to partial dissociation of Na^-. They are unlikely to arise from a mismatch in stoichiometry since the same behavior is seen for all (independently prepared) samples. The origin of the asymmetry is uncertain since it is not characteristic of solvated electrons in methylamine. In the dilute range ($n \geq 6$), the EPR spectra consist of a single line that is nearly symmetrical, although the asymmetry increases in the liquid state above 205 K. The asymmetry ratio is always below 1.4, and the Webb equation,[29] even to first order, cannot be used since such low values of A/B prevent convergence with so many adjustable parameters. However, when the particle size d becomes smaller than ten times the classical skin depth, the Webb equation can be represented as a linear combination of the dispersion and the absorption of a lorentzian function,[30]

$$\frac{dP}{dH} = c_1 \frac{1 - x^2}{(1 + x^2)^2} + c_2 \frac{2x}{(1 + x^2)^2} \tag{3}$$

in which $x = \gamma(H - H_0)T_2$. The coefficients c_1 and c_2 in both parts of the expression are related to the value of d/δ. The validity of this expansion was previously verified for colloidal potassium in frozen solutions[25] and in porous Vycor glass.[31] In our case, the EPR spectra of liquid samples at all temperatures for $n \geq 6$ could be fit to within experimental error by eq 3. The origin of asymmetry in this concentration region was first thought to be caused by the presence of colloidal sodium. It has been observed[38] that as the temperature of these systems is raised, there is the reversible formation of metallic sodium. If the particles were small enough to have rotational correlation

(36) Dye, J. L.; Nicely, V. A. *J. Chem. Educ.* **1971**, *48*, 443−448.
(37) Leclercq, F.; Damay, P. *Philos. Mag. B* **1988**, *57*, 61−74.
(38) McMills, L. E. H. Ph.D. Dissertation, Michigan State University, East Lansing, MI, 1989.

times comparable to T_2, both EPR line narrowing and the concentration and temperature dependence of the ^{23}Na chemical shift could occur by rapid exchange between Na^- and colloidal sodium metal. For the nanometer-size particles required to give such short rotational correlation times, however, the EPR line would be symmetric. The observed asymmetry cannot be from larger (micrometer sized) sodium particles, since the EPR line width of colloidal sodium in this size range is larger than 2 G at 90 K[39] and can be extrapolated to 5.6 ± 1 G at the temperatures used here, a value that is ten times broader than our signals. We conclude that the asymmetric EPR signal in the "dilute" range arises from moderate electronic conductivity of the electrons released by the partial dissociation of Na^-.

At high metal concentrations, liquid $Li(CH_3NH_2)_4$ is a quasi-metal while $Li(C_2H_5NH_2)_4$ is non-metallic in both the liquid and solid states. Now we find that $LiNa(CH_3NH_2)_n$ with n = 4 or 5 also behaves as a near-metal in the liquid state with a conductivity similar to that of $Li(CH_3NH_2)_4$. This is intriguing because, in the lithium−methylamine system, the electron is delocalized in an expanded lithium orbital or conduction band, while in the lithium−sodium−methylamine solutions, most of the "excess" electron density is located on the sodium atom to yield Na^-. The chemical shifts observed in the ^{23}Na NMR spectra are still *very* far from that of sodium metal, whose chemical shift is 1130 ppm[40]

A possible explanation is overlap of the wave functions of the highly polarizable and bulky sodide anions to form the metallic state according to the criterion of Herzfeld.[41] This approach considers the mutual polarization of an atom by the remaining atoms in the condensed phase, leading to a "dielectric catastrophe" as the metallic state is reached. The standard Clausius−Mosotti relationship for a non-metallic material relates the dielectric constant ϵ to the molar refractivity R by:

$$\frac{\epsilon - 1}{\epsilon + 2} = \frac{R}{V} \tag{4}$$

in which V is the molar volume in the condensed phase. As long as $R/V < 1.0$, ϵ is finite, but when R/V approaches unity, ϵ increases without limit. This indicates that the electrons that were previously bound become free and the sample becomes a metallic conductor. This simple distinction between non-metals and metals has been found to hold for a variety of systems.[42−44]

Neither the molar refractivity nor the molar volume of $LiNa(CH_3NH_2)_n$ are known experimentally. An estimate of R can be obtained from the molecular polarizability α through

$$R = {}^4/_3\pi N\alpha \tag{5}$$

in which N is Avogadro's number. It is likely that the sodide anion makes the largest contribution to α. The gas-phase polarizability of Na^- is 1090 au,[45] which yields R = 407 cm^3 mol^{-1}. The value of α in a liquid solution with the counterion $Li^+(CH_3NH_2)_4$ is not known, but calculations for crystalline Na^+(cryptand[2.2.2])Na^- indicate a reduction to about 400 au,[45] which would yield R = 150 cm^3 mol^{-1}. An upper limit on the molar volume uses the remarkably low density, 0.5 g cm^{-3}, of $Li(NH_3)_4$[4] to give a maximum value of 370 cm^3 mol^{-1} for a compound with n = 5 and 308 cm^3 mol^{-1} for n = 4. If the *gas-phase* polarizability and the *condensed-phase* molar volume are used, as was done in previous applications of the Herzfeld criterion,[41−44] R/V is greater than 1.0 even for the largest estimate of the molar volume. We conclude that, according to the original Herzfeld criterion, $LiNa(CH_3NH_2)_n$ is on the borderline of the transition to a metallic state when n becomes small. Measurement of the dielectric constant as a function of decreasing n would be required to verify an approach to the "polarization catastrophe".

If overlap of the Na^- wave function is not the cause of the observed high conductivity, we must conclude that the electrons released by dissociation of Na^- must be highly mobile—even more so than those in $Li(CH_3NH_2)_4$ since the electron concentration in the latter is much higher. Other alkali metal anions have higher polarizabilities than Na^-, so it would be useful to be able to prepare compounds of the type $LiM(CH_3NH_2)_n$, in which M is K, Rb, or Cs. Attempts to make such compounds have not yet been successful, but studies of such systems are underway.

Acknowledgment. The French authors thank NATO (Grant No. 0106/88), the Fondation de France, and the Fondation Norbert Segard for financial help at various levels in this study. The U.S. authors also acknowledge the NATO grant as well as support from the U.S. National Science Foundation under Solid-State Chemistry Grant Nos. DMR-90-17292 and DMR-94-02016 and the Michigan State University Center for Fundamental Materials Research. We thank Dr. Gregor Overney for help with computer programs.

JA952634P

(39) Edmonds, R. N.; Edwards, P. P.; Guy, S. C.; Johnson, D. C. *J. Phys. Chem.* **1984**, *88*, 3764−3771.
(40) Anderson, P. A.; Edwards, P. P. *J. Am. Chem. Soc.* **1992**, *114*, 10608−10618.
(41) Herzfeld, K. F. *Phys. Rev.* **1927**, *29*, 701−705.
(42) Herzfeld, K. F. *J. Chem. Phys.* **1966**, *44*, 429.
(43) Ross, M. Y. *J. Chem. Phys.* **1972**, *56*, 4651−4653.
(44) Edwards, P. P.; Sienko, M. J. *J. Chem. Educ.* **1983**, *60*, 691−696.
(45) Pyper, N. C.; Pike, C. G.; Edwards, P. P. *J. Am. Chem. Soc.* **1993**, *115*, 1468−1478.